Appendix A

Speckle Tracking Algorithm

Input atrioventricular valve (AV) annulus ends at the septal and lateral walls positions and the ventricle apex position are tracked temporally using Fourier domain cross-correlation (1, 2). Between sequential frames a subwindow of pixels centered around each position is taken. Each spatial subwindow pair, $w_1(x, y)$ and $w_2(x, y)$, is converted to the Fourier domain via the Fast Fourier Transform (FFT),

$$G_i(u, v) = \mathcal{F}\big(w_i(x, y)\big). \quad \text{Equation 1}$$

The Fourier Transforms for each pair are subsequently cross-correlated,

$$R(x, y) = \mathcal{F}^{-1}\big(G_1(u, v)\bar{G}_2(u, v)\big), \quad \text{Equation 2}$$

where $\mathcal{F}^{-1}$ is the inverse Fourier Transform (FT), (u, v) are wavenumbers proportional to spatial coordinates (x, y), and the overbar symbolizes the complex conjugate. The displacement between the pair is computed by the peak location of the cross-correlation R

$$(\Delta x, \Delta y) = argmax_{(x,y)}(R), \quad \text{Equation 3}$$

Each position is updated by adding the displacements to the current positions, which are then used as new centers for the next subwindow pair in the temporal image sequence.

Global Longitudinal Strain Algorithm

For each pair of co-registered frames containing the ventricle, a specialized correlation kernel is used to estimate GLSr between frames. The following steps are performed to calculate GLSr using the specialized kernel. First, the FFT for each frame in the pair is computed based on Equation 1. Next, the magnitudes of each FT are calculated, removing the phase content. Subsequently an interpolation is performed to render the FT magnitudes on a logarithm scale. Each re-scaled FT magnitude is then quartered into new subimages and their FFT is computed. The phase-filtered cross-correlation is then calculated for each subimage pair, like Equation 2, and their results are ensemble averaged. Finally, the displacements are found from cross-correlation peak based on Equation 3, which are converted from the logarithm scale to the image scale, returning a measurement for longitudinal strain. Each step is shown in Figure 1 of (3).

Unsupervised Segmentation Algorithm

Identifying the ventricle boundary with the unsupervised segmentation algorithm occurs in four steps: (1) image pre-processing, (2) path-finding with Dijkstra's algorithm using an echocardiogram specific cost-matrix, (3) post-processing, and (4) volume calculation.

Image pre-processing works to normalize the constrast-to-noise ratio (CNR), smooth added image noise, and transform the image onto a polar grid. These steps improve the reliability of the Dijkstra's algorithm in

segmenting the boundary. Image CNR normalization uses adaptive contrast enhancement, which is computed for each image pixel,

$$Im_{ACE}(x,y) = \frac{Im(x,y) - Im_{avg}}{Im_{max} - Im_{avg}}. \quad \text{Equation 4}$$

In Equation 4, Im_{ACE} is the ACE pixel intensity, Im is the raw pixel intensity, Im_{avg} is the average pixel intensity of a line from the AV valve ends to the ventricle apex, and Im_{max} is the maximum intensity in the entire image. Median filtering with an 11 x 11 pixel window is used to smooth the noise. The polar transformation, last in the image pre-processing, warps the image from a Cartesian grid (x, y) to a polar grid (ρ, θ) relative to the center of the ventricle (x_c, y_c), using the equations,

$$\rho = \sqrt{(x - x_c)^2 + (y - y_c)^2}, \theta = atan\left(\frac{y}{x}\right). \quad \text{Equation 5}$$

By transforming the ventricle image, the curve or path-finding of the ventricle simplifies the search for a curve that connects the two AV valve nodes through the ventricle apex. A cost-matrix for the performing the Dijkstra's algorithm is constructed by initially treating each pixel as a *graph-node*. A peak prominence--based cost was chosen; in this approach along each line of θ the local peak intensities $\left(\hat{I}\right)$ and their height compared to the local minimum $\left(\widehat{P}\right)$ are computed, which are used in the cost equation (C)

$$C = 15\left(\hat{P} + \hat{I}\right)^{-1}. \quad \text{Equation 6}$$

In order to reduce computation time, nodes larger than 1.25 the mean of C are discarded. The Dijkstra's algorithm (4) was used iteratively, allowing the method to detect the lowest cost for a limited number of lines of θ. This step size was varied from 2° to 14° in steps of 2°. The seven curves generated from the iterative processing were fit with a smoothing-spline radial basis function to produce a single representative curve, or the ventricle segmentation. This segmentation is converted back onto a Cartesian grid.

Each curve is post-processed with a boundary smoothing tool to ensure the segmentation appears physiologically consistent. This post-processing finds all possible paths within a neighboorhood of nodes in the curve, evaluates the gradients for all paths and the current path, selects the path with the smallest gradient. Two iterations are performed to ensure no over-smoothing occurs.

Doppler Vector Reconstruction Algorithm

The color Doppler vector reconstruction algorithm used in this work is based on the relationship between the flow rate and fluid rotation. The algorithm processes a single color Doppler frame by (1) converting the color signal to velocities, (2) segmenting the ventricle from the gray-scale signal and imposing boundary conditions, and (3) using a numerical solver to reconstruct the velocity field.

For each color Doppler recording, the user inputs the AV annulus end positions and ventricle apex position from the first recorded frame like the algorithms above. The user will also crop the velocity color

scale from the first recorded frame and provide its upper and lower velocity limits, in centimeters per second. A velocity range the same length as the color velocity scale is constructed.

A single frame is first separated into a color-signal image and a gray-scale image. This step avoids adding noise in further calculations and ensures only the blood flow signal is used in the reconstruction. Each pixel in the color-signal is converted to a velocity by converting its color value on the image velocity color scale to a velocity on the constructed velocity range. The output is a map of velocity measurements that correspond to the color-signal of the current color Doppler frame.

The gray-scale image is evaluated using the unsupervised segmentation algorithm and the current AV annulus end positions and apex position to obtain a segmentation curve. This curve is converted to a binary mask with the same dimensions as the map of velocity measurements. Velocity measurements along a line between the AV annulus end positions are used to impose inflow/outflow conditions for the solver,

$$\psi_{flow}(s) = \int_{s_0}^{s_a} u(s)\, d\xi + \psi_0. \qquad \text{Equation 7}$$

In equation 7, ψ_0 is the initial flow rate which we set to zero, ψ_{flow} is the flow rate a location along the line s, and s_0 and s_a are the annulus end positions of the line. A free-penetration condition is assumed along the ventricle walls to ensure flow rate is balanced, which is assumed to be linearly distributed,

$$\psi_{wall}(s) = f(s, u). \qquad \text{Equation 8}$$

The Doppler Vector Reconstruction (DoVeR) solver is used to reconstruct the 2D velocity vector field (5) using the boundary conditions and map of velocities. An initial fluid rotation source term, ω^0, is quantified. An initial error is provided, set to be infinite. DoVeR is an iterative reconstruction tool, so the error is checked against a threshold for each iteration; this threshold was set to 10^{-8}. The error is computed from the L2-norm of the difference between the current and previous iteration reconstructed vector fields,

$$\varepsilon = \frac{\|\mathbf{u}^n - \mathbf{u}^{n-1}\|}{\|\mathbf{u}^n\|}. \qquad \text{Equation 9}$$

So long as error is not minimized the iteration number, n, is increased and new flow rates through the ventricle ψ^n are computed from the fluid rotation ω^{n-1} by LU-decomposition of,

$$\ddot{\boldsymbol{D}}\psi^n = -\omega^{n-1}, \qquad \text{Equation 10}$$

where $\ddot{\boldsymbol{D}}$ is the second-order derivative operator of size $N \times N$ with a 3-point stencil size, and ω^{n-1} and ψ^n are $N \times 1$ vectors. The quantity N is the total number of points within the ventricle boundary. The reconstructed 2D velocity vector field, $\mathbf{u}^n$, is computed with,

$$\mathbf{u}^{\boldsymbol{n}} = [\mathrm{u}_x^n \quad \mathrm{u}_y^n] = \left[\dot{\boldsymbol{D}}_{\boldsymbol{y}}\psi^n \quad \dot{\boldsymbol{D}}_{\boldsymbol{x}}\psi^n\right], \qquad \text{Equation 11}$$

where $\dot{\boldsymbol{D}}_{\boldsymbol{x}}$ and $\dot{\boldsymbol{D}}_{\boldsymbol{y}}$ are first-order derivative operators of size $N \times N$ with 3-point stencil size for derivatives in x and y. All non-zero velocities from the input velocity map must remain constant in u_y^n to

further constrain the solver. Zero velocities from the input velocity map can be replaced but are threshold to ±10% of the maximum of the input velocity map. Finally, the fluid rotation ω^n is updated using the discrete formulation,

$$\omega^n = \dot{\boldsymbol{D}}_{\boldsymbol{x}} \mathrm{u}_y^n - \dot{\boldsymbol{D}}_{\boldsymbol{y}} \mathrm{u}_x^n. \quad \text{Equation 12}$$

Reconstruction post-processing

Post-processing the reconstructed 2D vector fields (Figure 1e) helps quantify ventricle flow efficiency. The vector fields are quantified using finite-differencing. Flow energy loss (EL) is calculated by,

$$EL = \int \left[2\left(\frac{\partial u_x}{\partial x}\right)^2 + 2\left(\frac{\partial u_y}{\partial y}\right)^2 + \left(\frac{\partial u_x}{\partial y} + \frac{\partial u_y}{\partial x}\right)^2 \right] dV, \quad \text{Equation 13}$$

where V is the volume of the region of flow, found by multiplying the 2D area of the ventricle by the AV valve diameter. Vortices are identified based on flow rotation, using the λ_{CI} criterion (6). The total vortex strength (VS) from this algorithm is,

$$VS = \sum \left| \int \omega dA \right|_{vortex}, \quad \text{Equation 14}$$

where A is the area of each identified vortex. The subscript indicates summation across all identified vortex structures. The 2D pressure field, P, inside the ventricles is computed using the pressure Poisson equation,

$$\nabla^2 P = \left(\frac{\partial u_x}{\partial x}\right)^2 + \left(\frac{\partial u_y}{\partial y}\right)^2 + 2\left(\frac{\partial u_x}{\partial y}\frac{\partial u_y}{\partial x}\right). \quad \text{Equation 15}$$

Neumann boundary conditions account for temporal variation of pressure. The solver reconstructs P using a least squares formulation, through an in-house algorithm described previously in (7). This analysis returns quantities for peak early and late AV valve velocities (E,A), EL, VS, and peak suction and reversal AV valve-to-apex pressure differences (ΔP).

References

1. Raffel M, Willert CE, Kompenhans J. Particle image velocimetry: a practical guide. 2007.

2. Friemel BH, Bohs LN, Trahey GE. Relative performance of two-dimensional speckle-tracking techniques: normalized correlation, non-normalized correlation and sum-absolute-difference. Proc. IEEE Ultrason. Symp. 1995;2:1481–1484.

3. Meyers BA, Brindise MC, Jani V, Kutty S, Vlachos PP. Direct estimation of global longitudinal strain from echocardiograms using a logarithm-scaled Fourier magnitude correlation. arXiv Prepr. arXiv2003.11672 2020.

4. Dijkstra EW. A note on two problems in connexion with graphs. Numer. Math. 1959;1:269–271.

5. Meyers BA, Goergen CJ, Segers P, Vlachos PP. Color-Doppler Echocardiography Flow Field Velocity Reconstruction Using a Streamfunction -Vorticity Formulation. eprint arXiv:1812.10580 2018:arXiv:1812.10580.

6. Jeong J, Hussain F. On the identification of a vortex. J. Fluid Mech. 1995;285:69–94.

7. Zhang J, Brindise MC, Rothenberger S, et al. 4D Flow MRI Pressure Estimation Using Velocity Measurement-Error based Weighted Least-Squares. IEEE Trans. Med. Imaging 2019.

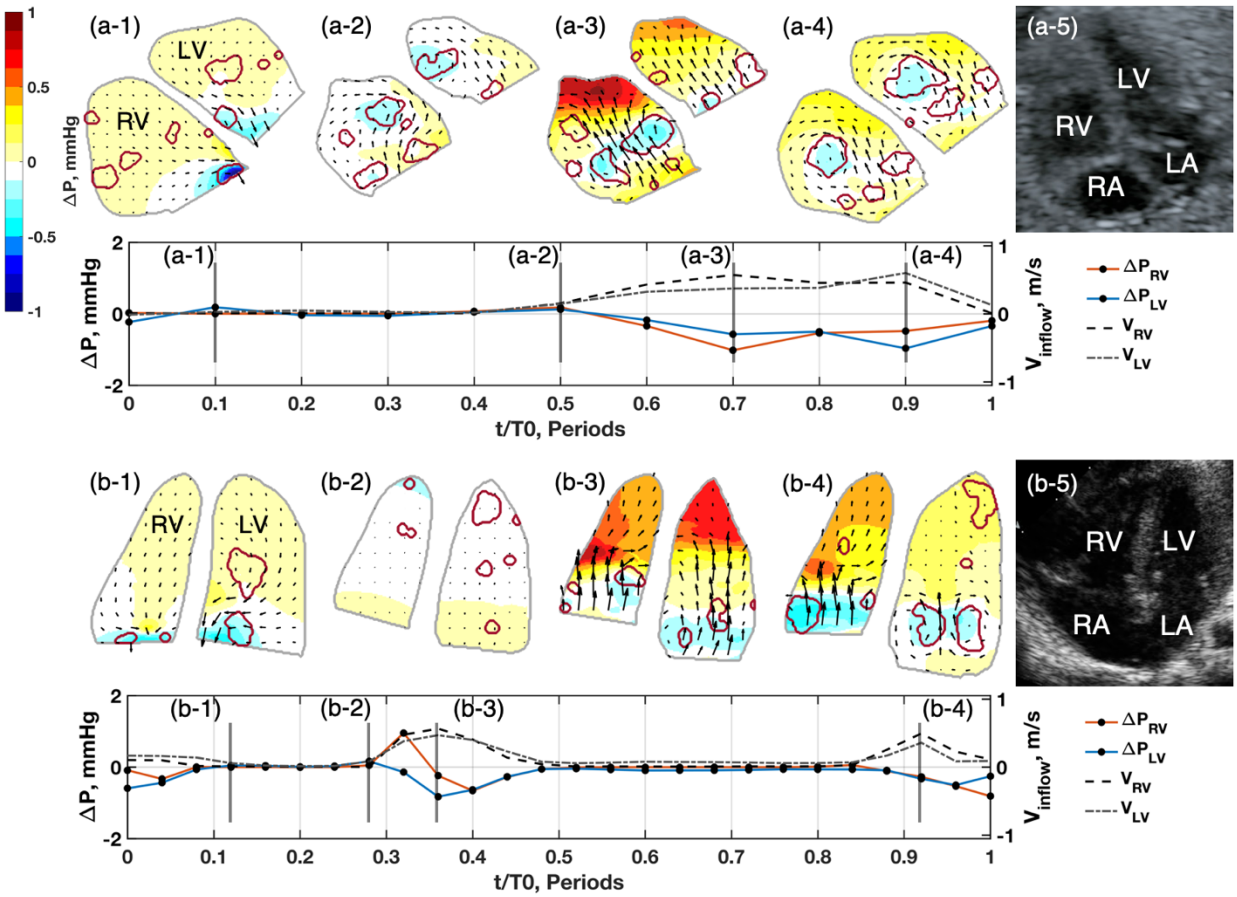

Figure 1: Velocity vector fields overlaid on estimated pressure contours for the healthy heart of (a) a fetus at 33-weeks gestation and (b) a baby at 0 weeks old.

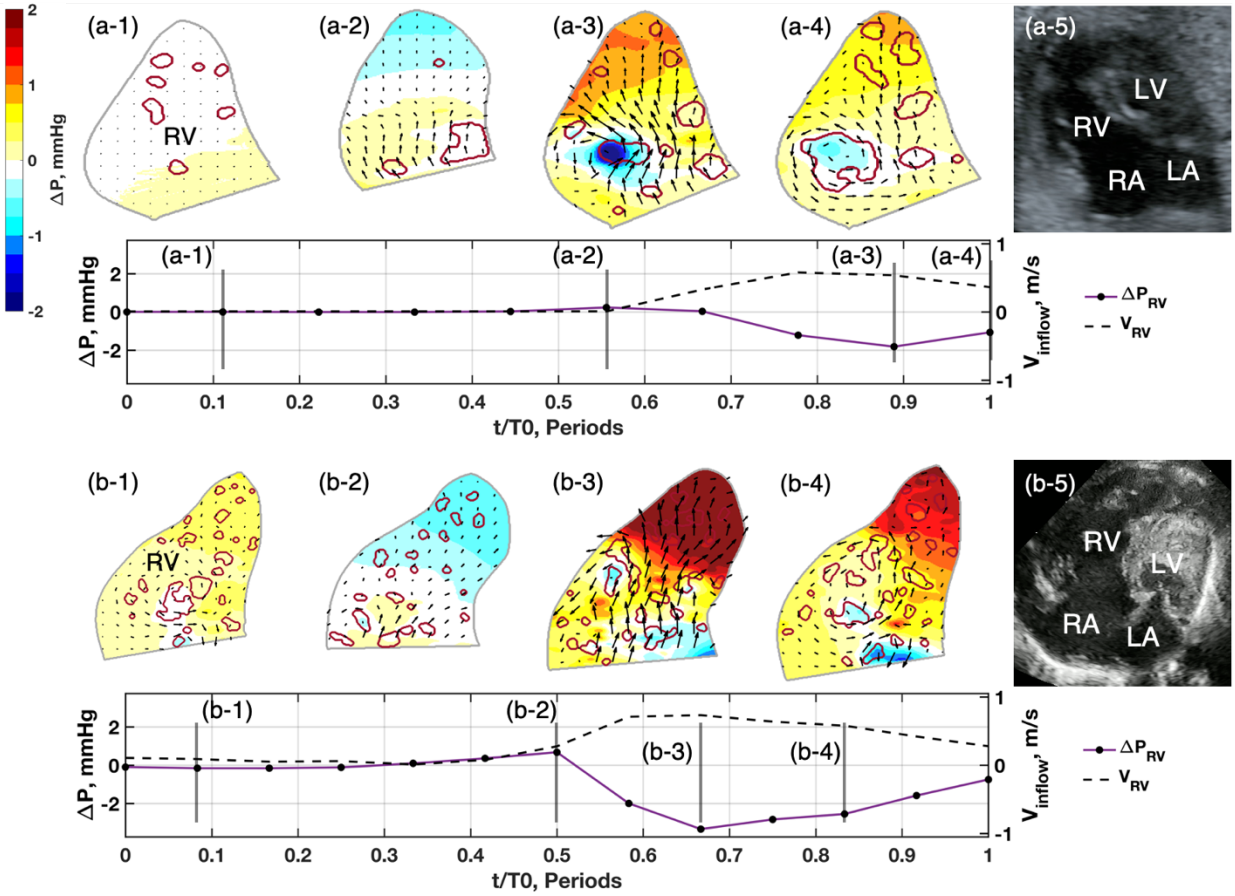

Figure 2:Velocity vector fields overlaid on estimated pressure contours for the single ventricle heart of (a) a fetus at 33-weeks gestation and (b) a baby at 0 weeks old.